International Journal of Science and Research (IJSR)
ISSN (Online): 2319-7064
Index Copernicus Value (2015): 78.96 | Impact Factor (2015): 6.391

Experimental and Theoretical Evaluation of new Quinazolinone Derivative as Organic Corrosion Inhibitor for Carbon Steel in 1M HCl Solution

Rehab Majed Kubba[1], Ahmad Shalaan Alag[2]

[1, 2]Department of Chemistry, College of Science, University of Baghdad, Baghdad, Iraq

Abstract: ***The inhibiting action of newly synthesised quinazolinone derivative namely 2-[(3-phenyl-4-oxo-3,4-dihydroquinazolinone-2-yl-thio) aceto] thiosemicarbazide (POQS), towards carbon steel corrosion in 1M HCl has been investigated at various concentration and different temperature using potentiodynamic polarisation, Scanning Electron Microscopy (SEM) and Energy Dispersion Spectroscopy (EDS) measurements. Polarisation curves showed that the compound acts as a mixed inhibitor, and the adsorption of the evaluated inhibitor obeys the Langmuir adsorption isotherm. SEM plots indicated that the presence of the inhibitor decreases the corrosion process of carbon steel in 1M HCl. Theoretically quantum mechanics calculations of the approximate semiempirical method PM3 and Density Functional Theory DFT of (B3LYP) with a 6-311++G (2d,2p) by using Gaussian-09 program were done to evaluate the structural, electronic and reactivity parameters of (POQS) in relation to their effectiveness as a corrosion inhibitor in vacuum and two liquid media (DMSO and H_2O) The calculated physical properties and quantum chemical parameters correlated to the inhibition efficiency all are studied and discussed at the equilibrium geometry.***

Keywords: Corrosion inhibitor, Quinazolinone derivative, 1M HCl solution

1. Introduction

Carbon steel corrosion has been a problem of enormous practical importance due to its high cost on the national economy. Despite its relatively limited corrosion resistance carbon steel is used in marine applications, petroleum production and refining, chemical processing, pipelines, mining, metal processing equipment, fossil fuel power and nuclear power plants. However, steels exposed to aqueous environments are strongly susceptible to corrosion due to their thermodynamic instability therein [1]. Mild steel is one of the major construction materials, which is extensively used in chemical and allied industries for the handling of acid, alkali and salt solutions [2]. Hydrochloric acid is the most difficult of the common acids to handle from the standpoints of corrosion and materials of constructions. This acid is very corrosive to most of the common metals and alloys [3]. Corrosion of metallic surfaces can be reduced or controlled by the addition of chemical compounds to the corrodent. This form of corrosion control is called inhibition and the compounds added are known as corrosion inhibitors. The inhibitors themselves form a protective film on the surface of the metal. It has been postulated that the inhibitors are adsorbed into the metal surface either by physical adsorption or chemisorptions [4]. Physical adsorption is the result of electrostatic attractive forces between the organic ions and the electrically charged metal surface. Chemisorption is the transfer, or sharing of the inhibitor molecule's charge to the metal surface, forming a coordinate-type bond. The adsorbed inhibitor reduces the corrosion rate of the metal surface either by retarding the anodic dissolution reaction of the metal, or by the cathodic evolution of hydrogen, or both [4]. Inhibitors can be used at pH values of acid from near neutral to alkaline.

Organic compounds containing electronegative functional groups and π-electrons in triple or conjugated double bonds are usually good corrosion inhibitors. Heteroatoms such as sulphur, phosphorus, nitrogen and oxygen as well as aromatic rings in their structure are the major adsorption centres. The efficiency of inhibitors depends on the characteristics of the environment in which it acts, the nature of the metal surface and electrochemical potential at the interface. The structure of the inhibitor itself, which includes the number of adsorption active centers in the molecule, their charge density, the molecule size, the mode of adsorption, the formation of metallic complexes and the projected area of the inhibitor on the metallic surface also has an effect on the efficiency of inhibitors [5]-[8].

One of the most important techniques that have been used to evaluate organic corrosion inhibitors is molecular modelling. Through correctly quantum mechanical calculations, it is possible to obtain structural parameters, such as the energies of the frontier molecular orbitals, the HOMO (highest occupied molecular orbital) and LUMO (lowest unoccupied molecular orbital), and the dipole moment….etc. These parameters influence the potential inhibition and are generally strongly correlated with the experimentally obtained protection efficiency [9]. Furthermore, DFT is considered a very useful technique to probe the inhibitor/surface interaction as well as to analyse the experimental data Thus, this technique is an important tool for pre-selecting possible corrosion inhibitors and studying the correlation between molecular structure and corrosion protection efficiency [10].

Quinazolinones are important heterocyclic with a wider range of microbial activities such as anti-malarial, anti-cancer, anti-inflammatory, anti-hypertensive, anti-convulsant, anti-HIV, etc [11]. Quinazolinone has two structural isomers, the 2-quinazolinone (A) and 4-quinazolinone (B). B isomer is the more common one [12] Figure 1.

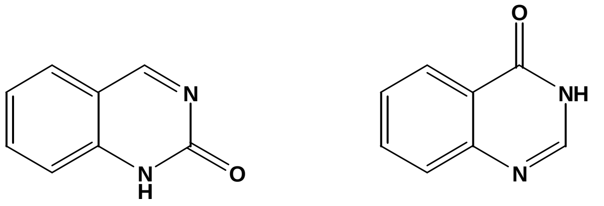

Quinazolin-2(1H)-one (A) **Quinazolin-4(3H)-one (B)**

Figure 1: The structural isomers of quinazolinone

2. Experimental part

2.1 Specimens Preparation

Rod of carbon steel (C45) with a chemical composition of metallic materials (in wt%) of (0.42-0.50)% C, 0.40% Si, (0.50-0.80)% Mn, 0.045% S, 0.40% Cr, 0.045% P, 0.40% Ni, 0.1% (Mo & Cr) and (97.31-97.96)% iron (Fe), cut into many specimens of carbon steel with 1cm diameter and 3 mm thickness, each specimen was polished with emery (80, 150, 220, 320, 400, 1000, 1200 and 2000) grades, washed thoroughly with deionized water, degreased with acetone, washed again with deionized water, and finally dried at room temperature.

2.2 Inhibitor synthesis

(a) Synthesis of 2-mercpto-3-phenyl-4(3H) quinazolinone [13].

A mixture of 8.228g (0.06mol) anthranilic acid, 7.22ml (0.06mol) of phenylisothiocyanate and 6ml of triethylamine in 100ml absolute ethanol was refluxed for 3hours. The reaction mixture was cooled to room temperature, poured into ice-cold water, stirred and filtered. The precipitate was recrystallized from ethanol to give crystals.

(b) Synthesis of S-(α-Chloroaceto-2-yl)-3-phenyl-4(3H) quinazolinone [14].

To a mixture of 3g (0.01mol) compound (a) in 16ml of dimethyl-formamide (DMF), 0.662g (0.01mol) of anhydrous potassium hydroxide dissolve in (9ml) of methanol and (1ml, 0.01mol) chloroacetylchloride added slowly. The mixture was refluxed for 4hours. left stirring overnight, then poured into an ice water for precipitation, filtered and recrystallized from ethanol to give white crystals.

(c) Synthesis of the inhibitor 2-[(3-phenyl-4-oxo-3,4-dihydroquinazolinone-2-yl-thio)Aceto] thiosemicarbazide (POQS) [15].

A mixture of 2g (0.006mol) of compound (b), 0.548g (0.006mol) thiosemicarbazide and 0.49g (0.006mol) of sodium acetate in 20ml absolute ethanol were placed in 100 ml round bottomed flask, refluxed for 10hours. The reaction mixture was filtered and poured into an ice water. The precipitate was filtered, dried and recrystallized from ethanol-water to give crystals.

2.3 Solutions preparation

a. Blank solution

For preparing ~1M of HCl, 87.290ml of concentrated HCl (35.4%, 1.18g/ml) diluted with deionized water in a volumetric flask of 1L containing 4ml DMSO which is used as an initial solvent in the preparation of the inhibitor solutions.

b. Inhibitor solutions

The solutions concentration of [1.298×10^{-5}M (5ppm), 2.597×10^{-5}M (10ppm), 5.194×10^{-5}M (20ppm), and 7.792×10^{-5}M (30ppm)] were prepared by dissolving 0.005g, 0.01g, 0.02g, and 0.03g of POQS respectively each in 4ml DMSO, transferred to a volumetric flask of 1L containing 87.290ml of HCl (35.4%, 1.18g/ml), completed the volume with de-ionized water.

2.4 Electrochemical measurements

The potentiostat set up include host computer, thermostat, magnetic stirrer, and Mat lab (Germany, 2000) potentiostat, galvanostat. The corrosion cell is (1L) capacity, made of Pyrex, it is a three compartments for working, a carbon steel working electrode with a $0.785cm^2$ surface area using to determine the potential of working electrode according to the reference electrode silver-silver chloride (Ag/AgCl, 3.0M KCl), a platinum auxiliary electrode with length (10cm). The working electrode was immersed in the test solution for 15 minutes to a establish steady state open circuit potential (E_{ocp}), then electrochemical measurements were performed in a potential range of (±200)mV and a scan rate of $5.0mV.s^{-1}$. All electrochemical tests have been performed in aerated solutions at 293 - 323K.

3. Results and Discussion

3.1 Synthesis of the compounds

(a) 2-mercpto-3-phenyl-4(3H)quinazolinone

Compound (a) was prepared via intermolecular cyclisation reaction of equimolar amounts of anthranilic acid and phenylisothiocyanate in present of triethylamine as a catalyst in ethanol. The mechanism [16] is shown in Scheme 1. Compound (a) was afforded with a yield of 89% and the melting point of 297 to 299°C.

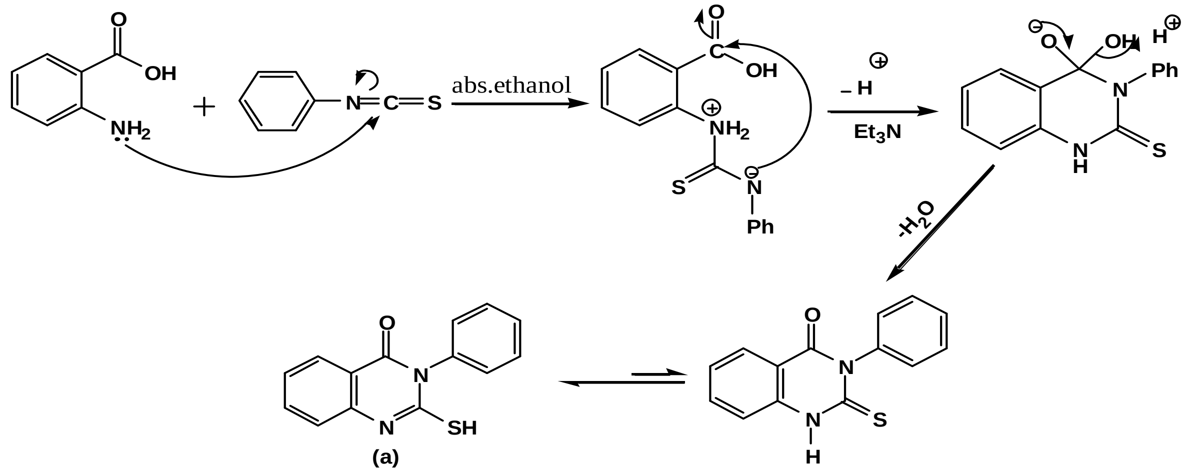

Scheme 1: The proposed mechanism for the preparation reaction of the compound (a)

(b) Preparation of S-(α-Chloroaceto-2-yl)-3-phenyl-4(3H) quinazolinone

Compound (b) was prepared by the nucleophilic substitution reaction of the compound (a) with chloroacetylchloride. This reaction is carried out in alcoholic potassium hydroxide solution to increase the nucleophilicity of sulfur atom in attacking molecule by forming potassium salt as an intermediate. Compound (b) was afforded as a white solid with a yield of 96% and m.p of 158-160°C. Also, silver nitrate alcoholic test confirmed the presence of chlorine group [17]. The mechanism [18] of the reaction is shown in Scheme 2.

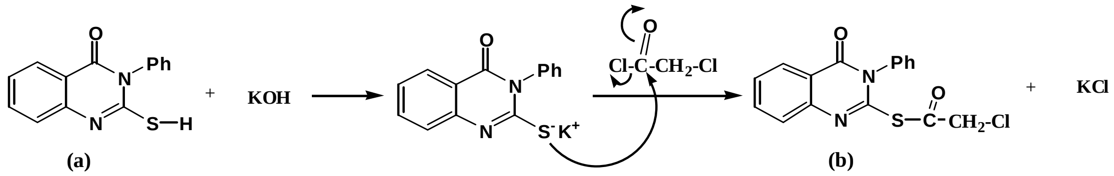

Scheme 2: The proposed reaction mechanism of preparation compound (b)

(c) Preparation of 2-[(3-phenyl-4-oxo-3,4-dihydroquinazolinone-2-yl-thio)aceto]thiosemicarbazide (POQS).

Compound (b) was converted to POQS Figure 2**a,** by reaction with thiosemicarbazide in absolute ethanol. POQS was afforded as a white solid with a yield of 83% and m.p of 239 to 240°C.

FTIR and HNMR spectrum for the newly prepared compound POQS

FTIR spectrum for the newly prepared quinazolinone derivative POQS shown absorption bands at 3447cm^{-1}, 3364cm^{-1} corresponding to the asymmetrical and symmetrical stretching vibration of NH_2, A sharp peak at 3245cm^{-1} referred to the characteristic stretching vibration of NH, 1735cm^{-1} to thioester C=O stretching, 1683cm^{-1} to amide C=O stretching, 1622 cm^{-1} to C=N stretching,1550, 1533, 1488 to C=C stretching and 1226 cm^{-1} referred to C=S stretching vibration. HNMR spectrum showed, 2.82 (d, 2H, CH_2); 3.40 (s, 2H, NH_2); 7.33-8.26 (m, 9H, Ar-H); 9.54 (d, 1H, N<u>H</u>).

3.2 Molecular modelling

PM3 semiempirical method and DFT utilizing Becke three-parameter and the connection useful of Lee, Yang and Parr (B3LYP) together with the standard double-zeta plus polarization 6-311++G (2d, 2p) [19]-[21], were carried out for figuring the optimize geometry of the investigate molecule in vacuum and two liquid media (DMSO and H_2O), implemented in the Gaussian 09 program package [22]. The final geometry of POQS is given in Figure 2b.

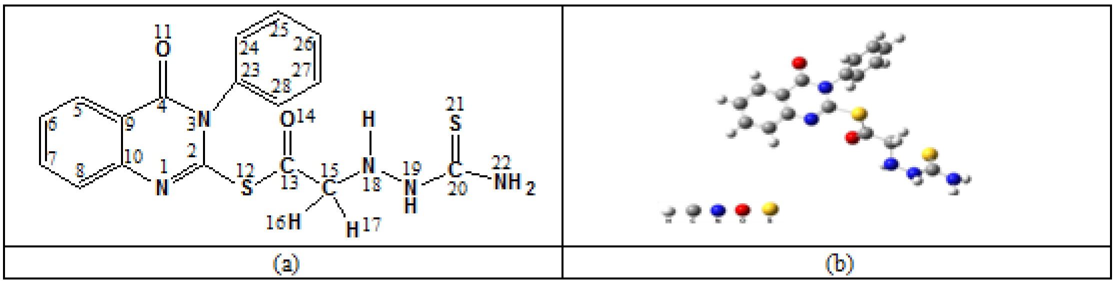

(a) (b)

Figure 2: a- Chemical structure of POQS**, b-** Equilibrium geometry of the POQS molecule calculated by DFT (B3LYP/6311++G (2d,2p)) method

3.2.1 Geometrical optimisation structure

The optimise structural parameters such as bond angles, bond distances and dihedral angles of the studied inhibitor are shown in Table 1, according to labels shown in Figure 2a The optimised geometrical structures observed to be the same in the three media (vacuum, DMSO, and H_2O). The longest bond length was observed for the S12-C13 bond ($1.824A^0$) due to the large bulky size of atom S comparing to others. The compound under investigation is not planar, Figure 2b. This result is confirmed by the values of the bond angles, cis and trans dihedral angles, Table 1.

Table 1: Calculated geometrical structure for POQS molecule by using DFT method.

Description bond length	***Bond length (Å)***	***Description bond angle***	***Bond Angle (deg)***	***Description dihedral angle***	***Dihedral angle (deg)***
N1-C2	1.278	N3C4O11	120.599	N1C2N3C4	0.017
N1-C10	1.384	N3C23C24	119.577	N1C2N3C23	179.711
C2-N3	1.389	C4N3C23	116.835	N1C2S12C13	77.615
C2-S12	1.799	C4C9C5	120.233	N1C10C9C4	0.867
N3-C4	1.421	C5C6C7	120.067	C2N1C10C8	178.410
N3-C23	1.446	C5C9C10	120.254	C2S12C13C15	179.742
C4-C9	1.464	C6C5C9	119.859	N3C4C9C10	0.878
C4=O11	1.214	C6C7C8	120.701	C2S12C13C15	179.742
C5-C6	1.380	C7C8C10	119.815	C4N3C2S12	-178.423
C5-C9	1.399	C8C7H	119.567	C4N3C23C28	90.885
C6-C7	1.402	C9C4O11	125.284	C4C9C5C6	179.755
C6-H	1.081	C9C5H	118.577	C5C6C7C8	0.058
C7-C8	1.381	C10C8H	118.454	C9C4N3C23	178.941
C8-C10	1.404	S12C13O14	125.338	S12C2N3C23	1.271
C9-C10	1.406	S12C13C15	110.941	S12C13C15H16	26.374
S12-C13	1.824	C13C15N18	108.661	S12C13C15H17	-91.968
C13=O14	1.194	C13C15H16	110.829	S12C13C15N18	146.515
C13-C15	1.516	C13C15H17	106.885	C13C15N18N19	176.855
C15-N18	1.471	O14C13C15	123.646	C13C15N18H	55.879
N18-N19	1.401	C15N18N19	113.698	O14C13C15H16	-156.607
N18-H	1.014	C15N18H	109.706	O14C13C15H17	85.049
N19-C20	1.365	H16C15H17	108.741	O14C13C15N18	-36.465
N19-H	1.007	H16C15N18	109.321	C15N18N19C20	-72.593
C20=S21	1.670	H17C15N18	112.393	C15N18N19H	91.685
C20-N22	1.366	N18N19C20	125.489	H16C15N18H	176.952
N22-H	1.008	N18N19H	113.329	H17C15N18N19	58.773
N22-H	1.005	N19N18H	107.947	N18N19C20S21	-6.971
C23-C24	1.389	N19C20S21	123.987	N18N19C20N22	173.451
C23-C28	1.388	N19C20N22	113.722	N19C20N22H	167.706
C24-C25	1.389	C20N19H	119.325	C20N19N18H	49.363
C25-C26	1.391	C20N22H	115.011	S21C20N19H	-170.390
C26-C27	1.390	S21C20N22	122.289	S21C20N22H	-156.249
C27-C28	1.390	HN22H	115.668	S21C20N22H	-11.878
C28-H	1.081	C23C24C25	119.465	N22C20N19H	10.032

Figure 3 shows the geometries optimisation of compound studied in the vacuum including HOMO and LUMO density distributions. HOMO mainly located on thiosemicarbazide moiety, this would indicate that the preferred actives sites for an electrophilic attack are located within the region around the nitrogen atoms belonging. Moreover, the electronic density of LUMO is distributed at the aromatic rings of quinazolinone moiety.

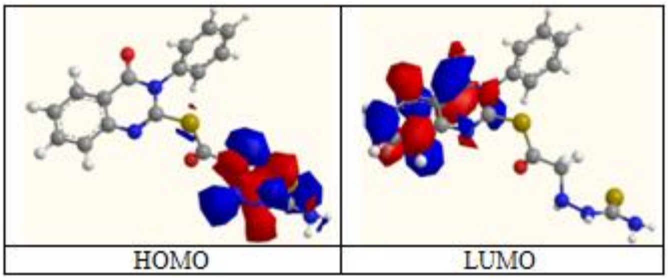

Figure 3: The Frontier molecule orbital density distributions of POQS inhibitor compound as calculated using DFT method. Red colour indicates the negatively charged lobe, blue colour indicates the positive charge lobe.

3.2.2 Global molecular reactivity

1. Molecular Orbital Energies

The HOMO energy (E_{HOMO}) is often associated with the electron donating ability of the molecule; therefore, inhibitors with high values of E_{HOMO} have a tendency to donate electrons to appropriate acceptor with low empty molecular orbital energy. Conversely, the LUMO energy (E_{LUMO}) indicates the electron-accepting ability of the molecule, the lowest its value the higher the capability of accepting electrons. The gap energy between the Frontier orbitals ($\Delta E_{HOMO-LUMO}$) is another important factor in describing the molecular activity, so when the gap energy decreased, the inhibitor efficiency is improved [23]. For POQS the E_{HOMO} in vacuum is (-6.217eV), decreased in both DMSO and H_2O solvents, the (E_{LUMO}) in the vacuum is (-

1.822eV), decreased in (DMSO and H_2O solvents and the value of $\Delta E_{HOMO-LUMO}$ is (4.395eV) in vacuum, be a higher in DMSO (4.471eV) and H_2O (4.473eV), indicating that the stability of the inhibitor in the solvents is more than that in the vacuum, Table 3.

2. Dipole moment

The dipole moment (μ in Debye) is a very important electronic parameter that results from the non-uniform distribution of charges on the various atoms in the molecule. The high value of dipole moment increases the adsorption between a chemical compound and metal surface [24]. Dipole moment for POQS inhibitor in vacuum and DMSO, H_2O solvents are (5.529, 7.867, 7.914 Debye) respectively, Table 3.

3. Ionisation potential energy IE

According to DFT-Koopman's theorem [25], the ionisation potential, **IE** can be approximated as the negative of the highest occupied molecular orbital (HOMO) energy.

$$IE = -E_{HOMO} \qquad (1)$$

Low values of IE increase the effectiveness of the inhibitor and inverse Versa. Good inhibitors with low energy of ionisation. The IE of POQS inhibitor in the vacuum is (6.217eV), increased in the DMSO (6.458eV) and H_2O (6.463eV) solvents, Table 4.

4. Electron affinity EA

EA is the amount of energy released when adding an electron to an atom or molecule. The **EA** is associated with (E_{LUMO}) by the relation in equation 2.

$$EA = -E_{LUMO} \qquad (2)$$

A high value of **EA** means less stable inhibitor. Particles with high electron affinity are good corrosion inhibitor. The electron affinity of POQS in the vacuum is (1.822eV), be a higher on using DMSO (1.987eV) and H_2O (1.990eV) solvents, Table 4.

5. Chemical Hardness (η)

It is a measure of the ability of atom or molecule to transfer the charge. Increasing (η) decreases the stability of molecule [26]. It is calculated by using equation 3 [27]:

$$\eta = \frac{IE - EA}{2} \qquad (3)$$

Compound possess a high value of (η) is considered to be a good inhibitor. (η) value for POQS in the vacuum is (2.197eV), be a lower in DMSO (2.235eV) and H_2O (2.236eV) solvents, Table 4.

6. Chemical Softness (S)

A measure of the flexibility of an atom to receive electrons **(S)**, was calculated by using equation 4:

$$S = \frac{1}{\eta} \qquad (4)$$

Molecules have a high value of S are considered to be a good inhibitor. The values of S in the vacuum is (0.455eV), the decrease in both DMSO and H_2O solvents to (0.447eV), Table 4.

7. The electronegativity (χ)

The ability of an atom or a group to pull electrons **χ** can be calculated by using equation 5 [28]:

$$\chi\ (\text{electronegativity}) = \frac{IE + EA}{2} \qquad (5)$$

High electronegativity indicates a good inhibitor. The calculated (**χ**) for POQS in the vacuum was found to be (4.019eV), increased in DMSO (4.222eV) and H_2O (4.226eV) solvents, Table 4.

8. Global electrophilicity index (ω)

ω is the measure of the stability of an atom after gaining an electron, Low value of (ω) meaning the molecule has a good inhibition. It is calculated by using equation 6.

$$\omega = \frac{\chi^2}{2\eta} \qquad (6)$$

The values of (ω) are shown in Table 4. In the vacuum is (3.676V), increased in DMSO (3.987eV) and in (H_2O) (3.993eV) solutions.

9. ΔN (Difference in number of electrons transferred)

The fraction of electrons transferred (ΔN) from an inhibitor to carbon steel surface was also calculated using a theoretical χ_{Fe} and η_{Fe} values for mild steel of 7.0eV mol^{-1} and 0.0eV mol^{-1}, respectively [29]. The ΔN values are correlated to the inhibition efficiency resulting from electron donation. According to Lukovits et al. study [30], if $\Delta N < 3.6$, the inhibition efficiency increases with increasing electron-donating ability at the metal surface. The obtained values of ΔN reported in Table 2 according to PM3 and Table 4 according to DFT; show that the POQS have the highest value of ΔN in the vacuum and solvent phase by the tendency of POQS molecule to receive the electrons from the metallic surface by S atoms in unoccupied orbital (3d). This ability increases the inhibition efficiency.

When two systems, Fe, and inhibitor, are brought together, electrons will flow from lower χ(inhibitor) to higher χ(Fe), until the chemical potentials become equal. The number of transferred electrons (ΔN) was calculated by using Equation 7 [31].

$$\Delta N = \frac{\chi_{Fe} - \chi_{inhib}}{[2(\eta_{Fe} + \eta_{inhib})]} \qquad (7)$$

Table 2: PM3 calculations of physical properties and quantum chemical parameters of POQS inhibitor at the equilibrium geometry.

ΔH^0_f kcal/mol	E_{HOMO} eV	E_{LUMO} eV	ΔE_{H-L} eV	μ Debye	IE eV	EA eV	η eV	χ eV	S eV	ω (eV)	ΔN
72.632	-9.023	-1.130	7.893	5.071	9.023	1.130	3.946	5.076	0.253	3.264	0.243

Table 3: DFT calculations for some physical properties of the POQS molecule at the equilibrium geometry in the three media (vacuum, DMSO, and H_2O)

Inhibitor medium	***Sym.***	***E_{HOMO} (eV)***	***E_{LUMO} (eV)***	***$\Delta E_{HOMO-LUMO}$ (eV)***	***μ (Debye)***	***E_{total} (eV)***
Vacuum	C1	-6.217	-1.822	4.395	5.529	-51097.804
DMSO	C1	-6.458	-1.987	4.471	7.867	-51098.516
H_2O	C1	-6.463	-1.990	4.473	7.914	-51098.527

Table 4: Quantum chemical parameters for the POQS molecule in the three media (vacuum, DMSO, and H_2O) as calculated using DFT method

Inhibitor medium	***IE (eV)***	***EA (eV)***	***η (eV)***	***S (eV)***	***χ (eV)***	***ω (eV)***	***ΔN***
Vacuum	6.217	1.822	2.197	0.455	4.019	3.676	0.678
DMSO	6.458	1.987	2.235	0.447	4.222	3.987	0.621
H_2O	6.463	1.990	2.236	0.447	4.226	3.993	0.620

3.2.3 Local reactivity for the 2-[(3-phenyl-4-oxo-3,4-dihydroquinazolinone-2-yl-thio)aceto] thiosemicarbazide (POQS)

For the purpose of establishing the active sites of the inhibitor calculated molecules, three influencing factors: natural atomic charge, distribution of frontier molecular orbital and indices. According to the classical chemical theory, all chemical interactions are either by electrostatic or orbital interactions. The local reactivity of the studied inhibitor is investigated using the DFT Mulliken charges population analysis which means the receptive centres of particles (nucleophilic and electrophilic centres). Along these lines, the particle areas where the electronic charge is high are chemically milder than the locales where the electronic charge is little, so the electron density assumes an imperative part in ascertaining the compound reactivity. Chemical adsorption communications are taking place either by electrostatic or orbital collaborations. For effortlessness, just the charges on the nitrogen (N), oxygen (O), sulfur (S), π electrons of the quinazolinone ring which are donating electrons to carbon steel surface and some carbon particles are exhibited. Consequently, the favored destinations for nucleophilic reactive sites are N1, C6, S12, O14, N18, S21 with the order of S21 > S12 > C6 > O14 > N18 > N1. For the most favored electrophilic reactive sites, that can accept electrons are C2 and C9 with the order of (C2 > C9) (which possess the highest positive charge on joining directly to the withdrawing aromatic ring) and (C4, C13, C20) atoms with the order of C13 > C20 > C4, which directly bonded to the oxygen and sulfur heteroatoms, Table 5. Consider the solvent effect, The values of the electronic charges for the nucleophilic and electrophilic reactive sites increase ongoing from vacuum to DMSO and H_2O solutions, making among adsorption by donating electron through sulfur atoms (S12, S21), the S atoms can donate and get the electron from the metal, because of possessing a lone pair of electrons and unfilled d orbital.

The negative charge centres could offer electrons to the Fe atoms to form a coordinate bond. The positive charge centres can accept electrons from 3d orbital of the Fe atom to form feedback bond, thus further strengthening the interaction of inhibitor and Fe surface

Table 5: DFT Mulliken charges population analysis for the calculated inhibitor molecule POQS in three media (vacuum, DMSO and H_2O).

Atom	***Electronic charge (ecu)***	***Atom***	***Electronic charge (ecu)***	***Atom***	***Electronic charge (ecu)***
N1	**-0.169V -0.258D -0.259W**	**C8**	**0.011V -0.005D -0.006W**	**C15**	**-0.183V -0.193D -0.194W**
C2	**0.382V 0.468D 0.470W**	**C9**	**0.247V 0.267D 0.268W**	**H16**	**0.116V 0.147D 0.147W**
N3	**-0.006V 0.048D 0.049W**	**C10**	**0.119V 0.147D 0.148W**	**N18**	**-0.210V -0.235D -0.235W**
C4	**0.107V 0.208D 0.211W**	**O11**	**-0.439V -0.522D -0.524W**	**N19**	**-0.161V -0.150D -0.150W**
C5	**-0.054V -0.061D -0.061W**	**S12**	**-0.420V -0.471D -0.472W**	**C20**	**0.175V 0.218D 0.219W**
C6	**-0.390V -0.442D -0.442W**	**C13**	**0.199V 0.247D 0.248W**	**S21**	**-0.432V -0.560D -0.562W**
C7	**-0.104V -0.130D -0.131W**	**O14**	**-0.278V -0.325D -0.326W**	**N22**	**-0.152V -0.182D -0.182W**

V: vacuum, D: dimethyl sulfoxide (DMSO), W: water, blue colour: increase in electronic charge to more positive, red colour: increase in electronic charge to more negative.

3.3 Corrosion measurement

3.3.1 Potentiostatic polarisation measurements

The electrochemical kinetics of metallic corrosion process can be characterised by determining at least three polarisation parameters, such as corrosion current density ($I_{corr.}$), corrosion potential ($E_{corr.}$) and Tafel slopes (ba and/or bc). The corrosion behaviour can be determined by a polarisation curve (E versus log I). The evaluation of the polarisation parameters leads to the determination of the corrosion rate (C.R) [32]. Using Tafel extrapolation method, it is possible to obtain the $I_{corr.}$ at the $E_{corr.}$ by the extrapolation of anodic and/or cathodic Tafel lines [33]. However, a prerequisite for this method to be used is that the graph of E versus log I must have at least one straight well-defined line [34]. Moreover, for an accurate estimation of $I_{corr.}$ by Tafel method, the linear regions should extend over about one decade on the log $I_{corr.}$ axis [35]. The error in the numerical values of Tafel slopes can reduce the accuracy of the values calculated for $I_{corr.}$ [36]. Potentiodynamic polarisation curves for carbon steel in 1M HCl at 293K in the absence and in the presence of different concentration of POQS are shown in Figure 4. The effect of increasing concentration and temperature on $E_{corr.}$, $I_{corr.}$, and Tafel slopes (bc and ba) are shown in Table 6, as well as protection efficiency %PE, surface coverage Θ and corrosion rate C.R which were calculated by using the following equations:

$$\%PE = 1 - \frac{I}{I_0} \times 100 \qquad (8)$$

I_o and I: the corrosion current densities in the absence and presence inhibitor, respectively.

$$\Theta = \frac{\%PE}{100} \qquad (9)$$

$$C.R = \frac{M}{n\,f\,\rho} \times I_{corr.} \qquad (10)$$

Where M is the atomic weight of the Fe metal (55.845g/mol), ρ is the density of the iron metal ($7.874 g/cm^2$), n is the charge number which indicates the number of electrons exchanged in the dissolution reaction and F is the Faraday constant (96.485 C/mol). Sometimes (M/n) ratio referred to be as an equivalent weight.

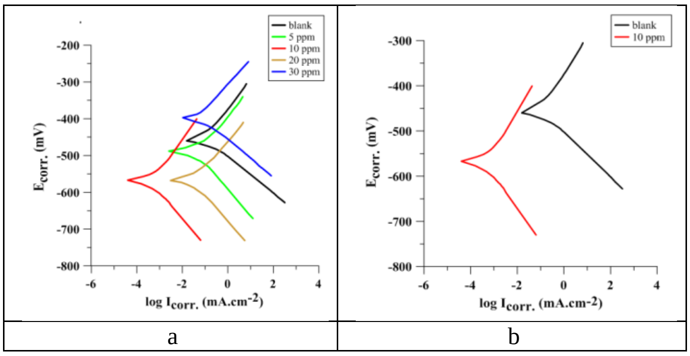

a b

Figure 4: Polarisation plots of carbon steel in 1M HCl for blank and inhibitor at a temperature of 293K (a) at various concentrations of POQS. (b) at the optimum concentration of POQS

Table 6: Electrochemical data of the carbon steel corrosion with 1M HCl at various concentrations of POQS and different temperature

Solun.	***T (K)***	***$E_{corr.}$ (mV)***	***$I_{corr.}$ ($\mu A.cm^{-2}$)***	***bc ($mV.dec^{-1}$)***	***ba ($mV.dec^{-1}$)***	***%PE***	***ϴ***	***C.R $mm.y^{-1}$***
Blank 1M HCl	293	-460.1	131.24	-120.3	102.1	....	....	1.521
	303	-457.6	182.19	-106.8	77.3	....	....	2.111
	313	-468.5	288.89	-132.7	94.2	....	....	3.348
	323	-441.1	528.72	-42.6	46.6	…….	……	6.128
POQS 5ppm	293	-488.3	29.95	-111.3	72.5	77.17	0.771	0.347
	303	-489.3	43.64	-108.6	73.6	76.04	0.760	0.505
	313	-499.1	70.40	-101.5	83.3	75.63	0.756	0.815
	323	-505.4	135.85	-85.4	74.0	74.30	0.743	1.574
POQS 10ppm	**293**	**-567.3**	**0.55**	**-215.4**	**234.9**	**99.58**	**0.995**	**0.006**
	303	**-533.3**	**0.83**	**-213.5**	**230.1**	**99.54**	**0.995**	**0.009**
	313	**-527.9**	**1.22**	**-236.9**	**244.7**	**99.57**	**0.995**	**0.014**
	323	**-517.8**	**2.73**	**-220.2**	**232.8**	**99.48**	**0.994**	**0.031**
POQS 20ppm	293	-568.7	30.19	-213.2	310.7	76.99	0.769	0.349
	303	-520.3	46.67	-71.7	76.3	74.38	0.743	0.540
	313	-521.9	72.51	-76.9	88.2	74.90	0.749	0.840
	323	-517.6	64.43	-90.7	76.6	87.81	0.878	0.746
POQS 30ppm	293	-397.6	32.87	-82.3	58.0	74.95	0.749	0.380
	303	-488.7	47.52	-53.8	55.2	73.91	0.739	0.550
	313	-494.9	75.55	-85.8	96.1	73.84	0.738	0.875
	323	-508.3	156.98	-79.5	79.6	70.30	0.703	1.819

3.3.2 Adsorption isotherm behaviour

Adsorption isotherms describe the behaviour of the inhibitor molecules and provide information about their interaction with the metal surface [37]. These isotherms require the degree of surface coverage (ϴ) for different inhibitor concentrations, which is calculated according to Equation 9. The adsorption behaviour of POQS was found to obey Langmuir isotherms. The Langmuir adsorption isotherm, given by Equation 11 [38], showed the best fit for each data set.

$$\frac{C_{inh.}}{\theta} = \frac{1}{K_{ads.}} + C_{inh.} \qquad (11)$$

Where, $C_{inh.}$ is the inhibitor concentration ($mol.L^{-1}$), $K_{ads.}$ is the adsorption/desorption equilibrium constant ($L.mol^{-1}$). The plot of $C_{inh.}/\Theta$ vs $C_{inh.}$ gave a straight line and the intercept represents ($1/K_{ads.}$) with a slight deviation of the slope from unity as shown in the correlation coefficient values, Figure 5. $K_{ads.}$ is related to the standard Gibbs free energy of adsorption ($\Delta G_{ads.}$), Equation 12 [39].

$$\Delta G_{ads.} = -2.303RT\,[\log 55.5K_{ads.}] \qquad (12)$$

Where R is the universal gas constant 8.314 $J.mol.^{-1}.K^{-1}$, T is the temperature (K), and 55.5 is the molar concentration of water ($mol.\ L^{-1}$).

The free energy of adsorption ($\Delta G_{ads.}$) was calculated from Equation 13.

$$\Delta G_{ads.} = \Delta H_{ads.} - T\Delta S_{ads} \qquad (13)$$

Where $\Delta H_{ads.}$, $\Delta S_{ads.}$ are the change in enthalpy and entropy of adsorption respectively, calculated from plotting Log $K_{ads.}$ vs (1/ T), Equation 14.

Equations 12 and 13 are combined to obtain Equation 14.

$$\text{Log } K_{ads.} = \frac{-\Delta H_{ads.}}{2.303\,RT} + \frac{\Delta S_{ads.}}{2.303\,R} + \text{Log } \frac{1}{55.5} \qquad (14)$$

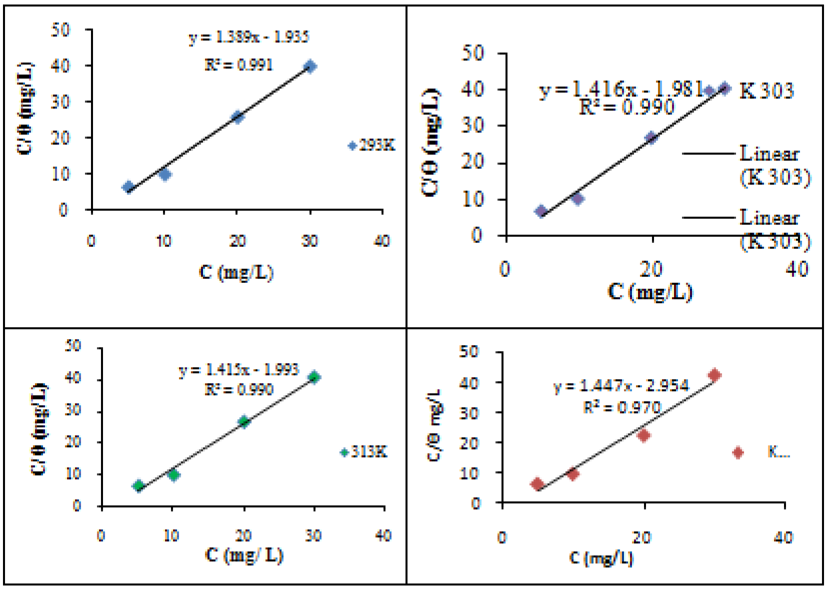

Figure 5: Langmuir isotherms plot for the adsorption of POQS on carbon steel at the temperature range (293,303,313 and 323K)

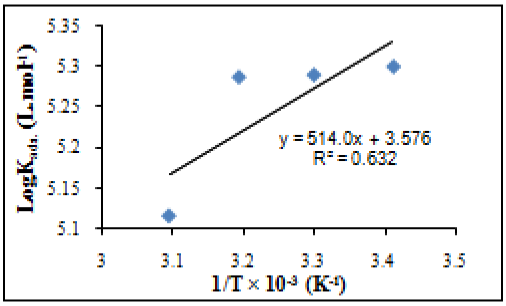

Figure 6: Plot of log $K_{ads.}$ versus 1/T for POQS inhibitor

The high values of $K_{ads.}$ indicate a strong interaction of POQS with the C-steel surface in 1M HCl [40], the optimum inhibition temperature is 293K, Table 7. The heterogeneous surface properties (i.e. flaws, impurities, cracks and vacancies) of the steel are responsible for the differential $\Delta G_{ads.}$ values obtained for POQS as the surface coverage value changes [41]-[43]. The negative values of $\Delta G_{ads.}$ ensure the spontaneity of the adsorption process and stability of the adsorbed layer on the carbon steel surface [44]. Furthermore, it is found that $\Delta G_{ads.}$ is slight decreases with temperature. Generally, $\Delta G_{ads.}$ values (0 to -20 kJ/mol.) are associated with electrostatic interactions between the charged molecules and the charged metal surface (physisorption), whereas those below -40 kJ/mol. involve the sharing or transfer of charge from the organic molecules to the metal surface to form a coordinate covalent bond (chemisorption) [45], [46]. In the present study, the value of $\Delta G_{ads.}$ is of -39.70 to -42.74 kJ.mol^{-1}. Figure 5 show the plotting of $C_{inh.}/\theta$ versus $C_{inh.}$, a straight line were obtained, proposing that the adsorption of the POQS inhibitor takes the Langmuir adsorption isotherm.

Table 7: Langmuir adsorption parameters of POQS with 1M HCl at different temperature and various concentration.

T (K)	$K_{ads.}$ (L.mol^{-1})	$\Delta G_{ads.}$ (kJ.mol^{-1})	$\Delta H_{ads.}$ (kJ.mol^{-1})	$\Delta S_{ads.}$ (kJmol^{-1}.K^{-1})	R^2
293	1.989×10^5	-39.69	-9.841	0.101	0.991
303	1.943×10^5	-40.71			0.991
313	1.931×10^5	-41.73			0.990
323	1.303×10^5	-42.75			0.970

The thermodynamic parameters got from the Langmuir isotherms slope represents $\Delta H_{ads.}$ and the intercept represents $\Delta S_{ads.}$ Figure 6. Through $\Delta H_{ads.}$ Table 7, the less value of $\Delta H_{ads.}$ meaning more stable adsorbent inhibitor. The negative value of $\Delta H_{ads.}$ indicates that the adsorption of inhibitor is an exothermic process [47]. Generally, an exothermic process signifies either physisorption or chemisorption while an endothermic process is attributable unequivocally to chemisorption [48]. ($\Delta S_{ads.}$) refer to random interaction, whenever it is less random the inhibitor is the best

3.3.3 Explanation for adsorption of POQS

Corrosion inhibition of carbon steel in 1M HCl solution by POQS inhibitor can be explained on the basis of molecular adsorption. It is a mixed complex type (comprehensive adsorption). This assumption is supported by data obtained for the temperature dependence of the inhibition process, which decreases with increasing temperature (physisorption) [49] and value of $\Delta G_{ads.}$ which suggested chemisorption Thus, we suppose the adsorption of POQS on carbon steel in 1M HCl is a complex in nature and predominantly physisorption.

3.3.4 Corrosion kinetic and thermodynamic activation parameters

Activation parameters were calculated for blank and optimum concentration (10ppm) of POQS. To decide the activation vitality of the corrosion procedure, activation parameters are taken at different temperatures (293, 303, 313, 323K) in the absence and presence of the 10ppm concentration of POQS. For calculating the activation parameters, Table 8, Arrhenius and Arrhenius transition state equations (15,16) were used respectively [50], [51].

$$\mathrm{Log\ C.R} = \mathrm{Log\ A} - \frac{\mathrm{Ea}}{2.303\ \mathrm{RT}} \qquad (15)$$

$$\mathrm{Log}\ \frac{\mathrm{C.R}}{\mathrm{T}} = \mathrm{Log}\ \frac{\mathrm{R}}{\mathrm{Nh}} + \frac{\Delta S^*}{2.303\,\mathrm{R}} - \frac{\Delta H^*}{2.303\,\mathrm{RT}} \qquad (16)$$

C.R is the corrosion rate (mm.y^{-1}**)**, R is the universal gas constant (8.314 J.mol^{-1}.K^{-1}), T is temperature (K), A is the Arrhenius pre-exponential factor (cm^{-2}.s^{-1}), Ea is the activation energy (minimum amount of energy required to initiate a chemical adsorption) (kJ. mol^{-1}), h is the Plank's constant (6.626 x 10^{-34} J.s^{-1}), N is the Avogadro's number (6.022 x 10^{23} mol^{-1}), ΔS* is the change in entropy of activation (kJ. mol^{-1}. K^{-1}) and ΔH* is the change in enthalpy of activation (kJ. mol^{-1}).

The activation energy Ea and Arrhenius factor A, at the absence and presence of the optimum concentration (10 mg/L) of POQS, was determined by linear regression between log C.R and 1/T, Figure 7. The results showed that the value of Ea for inhibited solution is higher than that for the uninhibited solution, suggesting that dissolution of carbon steel (C.S) is slow in the presence of inhibitor Table 8.

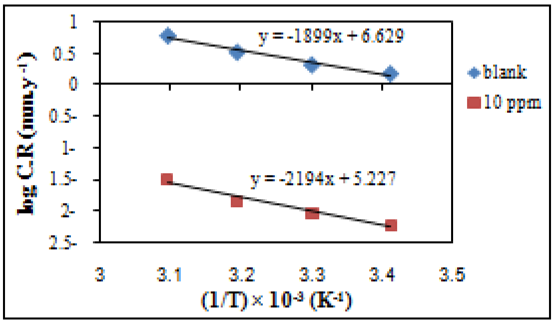

Figure 7: Plot of log C.R versus 1/T for the corrosion of C.S in 1M HCl at the optimum concentration (10 mg/L) of POQS inhibitor within the blank.

The enthalpy of activation ΔH* is obtained from the slope (-ΔH*/ 2.303R) obtained from plotting (log CR/T) vs. (1/T) with ΔS* which obtained from an intercept of [(log (R/ Nh) + (ΔS*/2.303R)] Figure 8. The positive sign of enthalpies ΔH* reflects the endothermic nature of dissolution process. ΔH* of the corrosion reaction on the C.S increasing in the presence of 10ppm of POQS.

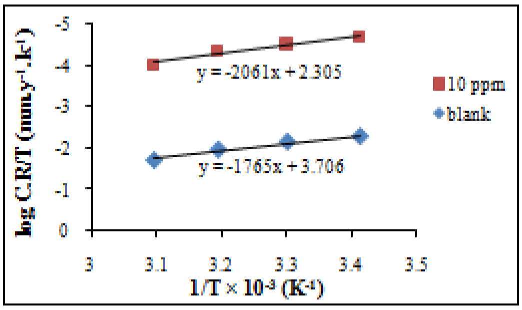

Figure 8: Arrhenius plots calculated from corrosion rate of C.S in 1M HCl in the absence and presence of the optimum concentration (10 mg/L) of POQS.

The entropy of activation ΔS* in the presence and absence of inhibitor has negative value, was affected when POQS was added at a temperature range (293-323)K Table 8, imply that the activated complex in the rate-determining step represents an association rather than dissociation step, it mean a decrease in disordering takes place on going from absence to the presence of inhibitor [52]. Activation free energy explains that the corrosion reaction of carbon steel is non-spontaneous and increase with increasing temperature, suppose that corrosion reaction increase with increasing temperature.

Table 8: Activation parameters for the C.S dissolution in 1M HCl in the absence and presence the optimum concentration of the inhibitor

Solution	*T (K)*	*ΔH* (kJ.mol^{-1})*	*ΔG* (kJ.mol^{-1})*	*ΔS* (kJ.mol^{-1}.K^{-1})*	*Ea (kJ.mol^{-1})*	*A (Molecule.cm^{-2}. s^{-1})*
Blank 1M HCl	293	33.795	70.889	-0.127	36.360	2.562 × 10^{30}
	303		72.155			
	313		73.421			
	323		74.687			
POQS 10 ppm	293	39.462	84.416	-0.153	42.009	1.015 × 10^{29}
	303		85.950			
	313		87.485			
	323		89.019			

3.4 Scanning electron microscopy (SEM) for carbon steel surface with 1M HCl in the absence and in the presence of POQS

SEM image of carbon steel surface in the absence of inhibitor reveals that it consists of spherical particles formed, with characteristic uniform corrosion of carbon steel in 1M HCl solution and a presence of deformities, Figure 9a. In the present of POQS, the morphology of carbon steel surfaces is quite different from it in the absence of POQS, the specimen surfaces had been smoother. It is possible that the inhibitor particles grow inside the C.S pore channels forming a film distributed in a homogenous way on the whole surface. This may be interpreted as due to the adsorption of the POQS on the C.S surface incorporating into the passive film in order to block the active site present on the inhibited surface, or due to the involvement of inhibitor molecules in the interaction with the reaction sites of C.S surface, resulting in a decrease in the contact between carbon steel and the aggressive medium and sequentially exhibited excellent inhibition effect [53], [54] Figure 9b. The scale bar for these images is 500 µm and the energy of the acceleration beam was 20kV.

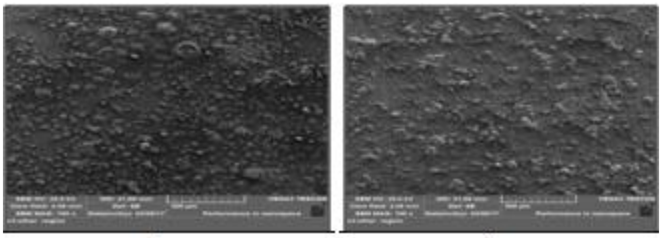
a b

Figure 9: SEM image for C.S surface with 1M HCl solution in the absence of POQS and, b- in the presence of (10ppm) POQS.

3.5 Energy Dispersion Spectroscopy (EDS) Studies

The EDS spectrum was used to determine the elements present on the surface of carbon steel uninhibited and inhibited with 10ppm POQS in the 1M HCl solution Figure 10. The analysis data showed that the Fe atoms decrease in the presence of POQS due to inhibitor's film covered the specimen surface. O atoms were also decreased in the presence of inhibitor in 1M HCl solution which represent the passive film of Fe_2O_3 and that indicate decrease corrosion of carbon steel. EDS spectrum displays the characteristic peaks (C, Mn and Cl) ascribed to general corrosion in 1M HCl solution. A comparable elemental distribution is shown in Table 9.

Table 9: Surface composition (weight %) of carbon steel alloy after immersion in 1M HCl without and with 10ppm of the quinazolinone derivative

Medium	*Fe*	*O*	*C*	*Cl*	*Mn*
Blank	66.4	30.9	----	1.6	1.1
POQS (10 ppm)	64.2	24.9	9.7	----	1.3

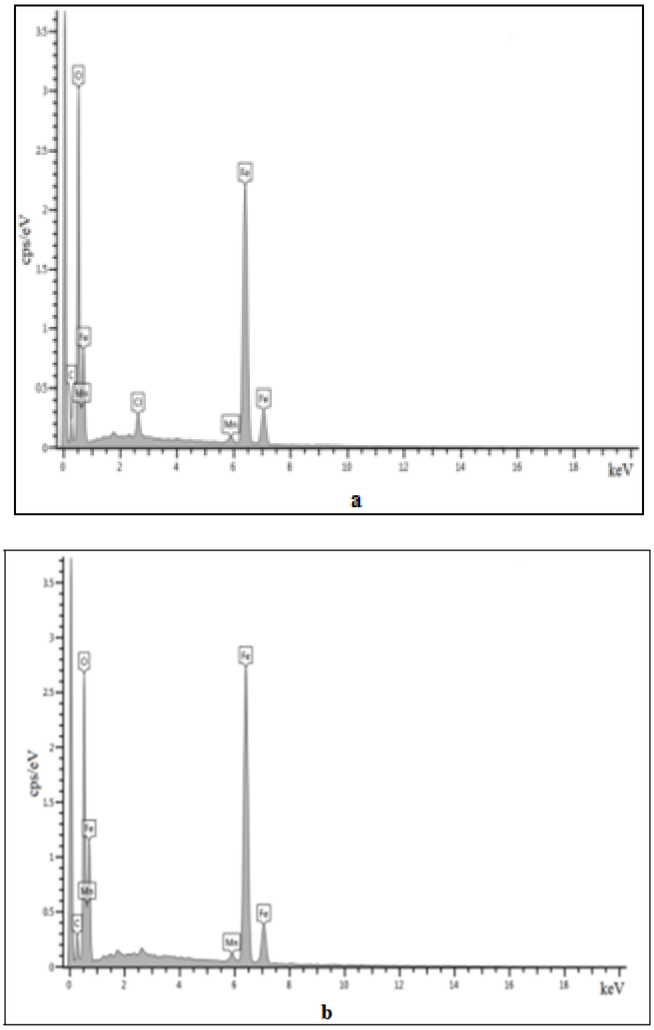

a

b

Figure 10: EDS analysis on C.S with 1M HCl, a- in the absence of inhibitor and b- in the presence of inhibitor (10ppm) POQS

4. Conclusion

- Quinazolinone derivative was found to be an effective inhibitor for carbon steel corrosion in 1M HCl solution.
- Protection efficiency decreases with an increased temperature; the optimum concentration of POQS for inhibition is 10ppm.
- The potentiodynamic polarisation measurements showed that the inhibitor can be classified as a mixed inhibitor in 1M HCl.
- The adsorption of the compound POQS on Mild steel surface follows the Langmuir adsorption isotherm model.
- The high $K_{ads.}$ values indicate a strong interaction between the inhibitors and the mild steel surface. The adsorption of POQS on the carbon steel surface involves both physisorption and chemisorption (comprehensive adsorption) but physisorption is the predominant mode of adsorption. This assumption is supported by data obtained from temperature dependence of inhibition process, which shows that the protection efficiency of the POQS studied decreases with increase in temperature (physisorption) and $\Delta G_{ads.}$ values obtained for the POQS on carbon steel in 1M HCl solution range of -39.70 to -42.74 kJ mol^{-1} (chemisorption).

Quantum chemical parameters for the investigated compound were calculated to provide further insight into the mechanism of POQS inhibition of the corrosion process. Both PM3 and DFT methods show that the inhibitor molecule is efficient for the corrosion inhibition.

References

[1] A. Tosun, M. Ergun, Protection of corrosion of carbon steel by inhibitors in chloride containing solutions, G. U. Journal of Science 19(3) (2006) 149-154.
[2] D.S. Shetty, P. Shetty, and S.H. Nayak, The inhibition action of N-(furfuryl)-N'-phenyl thiourea on the corrosion of mild stell in acid media, Journal of the Serbian Chemical Society, 71(10) (2006) 1073-1082.
[3] M.G. Fontana, Corrosion Engineering. 3rd Ed., McGraw-Hill Book Company, New York, (1987) 346.
[4] D. Benjamin, and A. Richard, Corrosion Prevention and Control: A Program Management Guide for Selecting Materials, Alion Science and Technology 246 (2006) 79.
[5] G.H. Naeimi, N. Soltani, M. Behpour, M. Sayed, Corrosion inhibition of mild steel in hydrochloric acid solution by some double Schiff bases. Corrosion Science, 52(4) (2010) 1351-1361.
[6] I. Obot, and N. Obi-Egbedi, Inhibitory effect and adsorption characteristics of 2, 3-diaminonaphthalene at aluminum/ hydrochloric acid interface: experimental and theoretical study, Surface Review and Letters 15(06) (2008) 903-910.
[7] I.B. Obot, N.O. Obi-Egbedi, S.A. Umoren, E.E. Ebenso, Synergistic and antagonistic effects of anions and Ipomoea invulcrata as green corrosion inhibitor for aluminium dissolution in acidic medium, Int. J. Electrochem. Sci. 5(7) (2010) 994-1007.
[8] I. Obot, and N. Obi-Egbedi, Adsorption properties and inhibition of mild steel corrosion in sulphuric acid solution by ketoconazole: experimental and theoretical investigation. Corrosion Science, 52(1) (2010). 198-204.
[9] M.K. Awad, M.R. Mustafa, M.M.A. Elnga, Computational simulation of the molecular structure of some triazoles as inhibitors for the corrosion of metal surface, J. Mol. Struct. THEOCHEM 959 (2010) 66–74.
[10] A.Y. Musa, R.T.T. Jalgham, A.B. Mohamad, Molecular dynamic and quantum chemical calculations for phthalazine derivatives as corrosion inhibitors of mild steel in 1 M HCl, Corros. Sci. 56 (2012) 176–183.
[11] K. Tereshina, H. Shimamura, and M. Sato, Synthesis and characterization of some diazocompounds. Chem. and Pharma. Bulletin, 45 (1995) 2021-2030.
[12] A. Chawla, and C. Batra, Recent advances of quinazolinone derivatives as marker for various biological activities. Int. Res. J. Pharm. 4 (3) (2013) 49-58.
[13] A. Alafeefy, Some new quinazolin-4(3H)-one derivative, synthesis and antitumor activity, J. Saudi Chem. Soc. 18 (2011) 337-343.
[14] M. Suaad, Al-Majidi, Synthesis, Characterization and Evaluation of Antimicrobial Activity of Several New N-Substituted Carbazole, J. Al-Nahrain Un.16(4) (2013).67-79.
[15] W. Wafaa, Synthesis of some new derivatives of 1,2,4-triazole and thiazole from 1,2,3,4-tetrahydrocarbazole and study their biological activity, J. Al-Nahrain Univ. Sci. 13(2) (2010) 54-62.
[16] J. Joule, and M. Mills, (Heterocyclic Chemistry) 5th ed., John Wiley & Sons, Inc. USA (2010).
[17] R. Shriner, R. Fuson, D. Cartin, and T. Morril, (The systematic Identification of Organic Compounds) 8th ed., John Wiley and Sons, New York, USA (1980).
[18] J. March, (Advanced Organic Chemistry) 3rd ed., Wiley, New York, USA(1985).
[19] R.G. Parr, and W. Yang, Density Functional Theory of Atoms and Molecules. 1ST Edn., 1989 Oxford University Press: New York,
[20] A.D. Becke Density-functional thermochemistry. III. The role of exact exchange. J. Chem. Phys. 98 (1993) 5648-5652.
[21] C. Lee, W. Yang, and R.G. Parr, Development of the Colle-Salvetti correlation energy formula into a functional of the electron density, Phys. Rev. B 41 (1988) 785-789.
[22] Frisch, M.J. Trucks, G.W. Schlegel, H.B. Scuseria, G.E. Robb,M.A. Cheeseman, J.R. Montgomery, J.A. Jr., Vreven, T. Kudin, K.N. Burant, J.C. Millam, J.M. Iyengar, S.S. Tomasi, J. Barone, V. Mennucci, B. Cossi, M. Scalmani, G. Rega, N. Petersson, G.A. Nakatsuji, H. Hada, M. Ehara, M. Toyota, K. Fukuda, R. Hasegawa, J. Ishida, M. Nakajima, T. Honda, Y. Kitao, O. Nakai, H. Klene, M. Li, X. Knox, J.E. Hratchian, H.P. Cross, J.B. Bakken, V. Adamo, C. Jaramillo,J. Gomperts, R. Stratmann,R. E. Yazyev, O.Austin, A.J. Cammi,R. Pomelli,C Ochterski, J.W. Ayala, P.Y. Morokuma, K. Voth, G.A. Salvador, P. Dannenberg, J.J. Zakrzewski, V.G. Dapprich, S. Daniels, A.D. Strain, M.C. Farkas, O. Malick, D.K. Rabuck, A. D. Raghavachari, K Foresman, J. B. Ortiz,J. V Cui, Q. Baboul, A. G. Clifford, S. Cioslowski, J. Stefanov, B.B. Liu, G. Liashenko, A. Piskorz, P. Komaromi, I. Martin, R.L. Fox, D.J. Keith, T. Al-Laham, M.A. Peng, C.Y. Nanayakkara, A. Challacombe, M. Gill, P.M. W. Johnson B. Chen, W. Wong, M.W. Gonzalez, C.and Pople, J.A. 2009. Gaussian 03, Gaussian. Inc. Pittsburgh PA.
[23] J. Zhang, J. Liu, W. Yu, Y. Yan, L.You & L. Liu, , Molecular modeling of the inhibition mechanism of 1-(2-aminoethyl)-2-alkyl-imidazoline, Corrosion Science, 52(6) (2010) 2059-2065.
[24] H. Wang, X. Wang, H. Wang, L. Wang, and A. Liu, DFT study of new bipyrazole derivatives and their potential activity as corrosion inhibitors, Journal of Molecular Modeling, 13(1) (2007) 147-153.
[25] T. Koopmans, Über die Zuordnung von Wellenfunktionen und Eigenwerten zu den einzelnen Elektronen eines Atoms, Physica 1(1-6) (1934) 104-113.
[26] C. Speicher, and R. Dreizler, Density functional App: roach to quantum hadrodynamics: theoretical foundations and construction of extended thomas- fermi models, Annals of Physics, 213 (1998) 312-354.
[27] R.G. Parr, and R.G. Pearson, Absolute hardness: companion parameter to absolute electronegativity, J. Am. Chem. Soc. 105 (1983) 7512-7516.
[28] R.G. Pearson, Absolute electronegativity and hardness application to inorganic chemistry. Inorganic Chemistry. 27, 4 (1988) 734–740.

[29] H. Chermette, Chemical Reactivity Indexes in Density Functional Theory, J. Comput. Chem. 20 (1999) 129-154

[30] I. Lukovits, E. Kalman, and F. Zucchi, Corrosion inhibitors—correlation between electronic structure and efficiency, Corrosion, 57(1), 2001, 3-8.

[31] P. Zhao, Q. Liang, and Y. Li, Electrochemical, SEM/ EDS and quantum chemical study of phthalocyanines as corrosion inhibitors for mild steel in 1 mol/l HCl, Applied Surface Science, 252(5) (2005) 1596-1607.

[32] N. Perez, Electrochemistry and Corrosion Science, Kluwer Academic Publishers, Boston, 412 (2004).

[33] E. Poorqasemi, O. Abootalebi, M. Peikari, F. Haqdar, Investigating accuracy of the Tafel extrapolation method in HCl solutions, Corros. Sci. 51 (2009) 1043– 1054.

[34] S. Wolynec, Técnicas Eletroquímicas em Corrosão, Editora da Universidade de São Paulo, São Paulo, 2003.

[35] H.J. Flitt, D.P. Schweinsberg, Evaluation of corrosion rate from polarization curves not exhibiting a Tafel region, Corros. Sci. 47 (2005) 3034–3052.

[36] M.A. Amin, S.S.A.E. Rehim, H.T.M. Abdel-Fatah, Electrochemical frequency modulation and inductively coupled plasma atomic emission spectroscopy methods for monitoring corrosion rates and inhibition of low alloy steel corrosion in HCl solutions and a test for validity of the Tafel extrapolation method, Corros. Sci. 51 (2009) 882–894.

[37] HM. Abd El-Lateef, VM. Abbasov, LI. Aliyeva, EE. Qasimov, IT. Ismayilov, Inhibition of carbon steel corrosion in CO_2-saturated brine using some newly surfactants based on palm oil: experimental and theoretical investigations, Mater Chem. Phys. 142(2–3) (2013) 502–12.

[38] X. Li, S. Deng, H. Fu, Allyl thiourea as a corrosion inhibitor for cold rolled steel in H3PO4 solution, Corros. Sci. 55 (2012) 280–288.

[39] S.D. Shetty, P. Shetty, H.V.S. Nayak, The inhibition action of N-(furfuryl)-N- phenyl thiourea on the corrosion of mild steel in hydrochloric acid medium, Mater. Lett. 61 (2007) 2347–2349.

[40] S. Safak, B. Duran, A. Yurt, G. Turkogˇlu, Schiff bases as corrosion inhibitor for aluminium in HCl solution, Corros. Sci. 54 (2012) 251–259.

[41] OK. Abiola, Adsorption of 3-(4-amino-2-methyl-5-pyrimidyl methyl)-4-methyl thiazolium chloride on mild steel, Corros. Sci. 48 (2006) 3078–90.

[42] BB. Damaskin, AN. Frumkin, Adsorption of molecules on electrodes. London: Wiley Interscience; (1971) p.36.

[43] M. Susuki, Adsorption engineering, Amsterdam, Elsevier, (1990) 52.

[44] J. Cruz, R.Martinez, J.Genesca, E.G.Ochoa, Experimental and theoretical study of 1-(2-ethylamino)-2-methylimidazoline as an inhibitor of carbon steel corrosion in acid media, J. Electroan. Chem. 566(1) (2004) 111-121.

[45] M.J. Bahrami, S.M.A. Hosseini, P. Pilvar, Experimental and theoretical investigation of organic compounds as inhibitors for mild steel corrosion in sulfuric acid medium, Corros. Sci. 52 (2010) 2793–2803.

[46] M. Behpour, S.M. Ghoreishi, N. Mohammadi, N. Soltani, M. Salavati-Niasari, Investigation of some Schiff base compounds containing disulfide bond as HCl corrosion inhibitors for mild steel, Corros. Sci. 52 (2010) 4046–4057.

[47] G. K. Gomma, M. H. Wahdan, Schiff bases as corrosion inhibitors for aluminium in hydrochloric acid solution, Materials chemistry and physics 39(3) (1995) 209-213.

[48] W. Durnie, R. DeMarco, A. Jefferson, B. Kinsella, Development of a structure-activity relationship for oil field corrosion inhibitors, J. Electrochem. Soc. 146(5) (1999) 1751-1756.

[49] M.M. Solomon, S.A. Umoren, I.I. Udosoro, A.P. Udoh, Inhibitive and adsorption behaviour of carboxymethyl cellulose on mild steel corrosion in sulphuric acid solution, Corros. Sci. 52(4) (2010) 1317-1325

[50] M. Dahmani, A. Et-Touhami, S.S. Al-Deyab, B. Hammouti, A. Bouyanzer, Corrosion Inhibition of C38 Steel in 1M HCl: A Comparative Study of Black Pepper Extract and Its Isolated Piperine, Int. J. Electrochem. Sci., 5(8) (2010) 1060-1069.

[51] A. Singh, V. K. Singh, M. A. Quraishi, Effect of fruit extracts of some environmentally benign green corrosion inhibitors on corrosion of mild steel in hydrochloric acid solution, J. Mater. Environ. Sci. 1(3) (2010) 162-174.

[52] N. Soltani, M. Behpour, S.M. Ghoreishi, H. Naeimi, Corrosion inhibition of mild steel in hydrochloric acid solution by double Schiff bases. Corros. Sci. 52 (4) (2010) 1351–1361.

[53] R.A. Prabhu, T.V. Venkatesha, A.V. Shanbhag, G.M. Kulkarni, R.G Kalkhambkar, Inhibition effects of some Schiff's bases on the corrosion of mild steel in hydrochloric acid solution. Corros. Sci. 50(12) (2008) 3356-3362.

[54] G. Moretti, G. Quartarone, A. Tassan, A. Zingales, Inhibition of mild steel corrosion in 1N sulphuric acid through indole, Materials and Corrosion, 45(12) (1994) 641-647.

Author Profile

Rehab Majed Mohammad rasheed received Ph.D degree. Prof. Dr. Physical Chemistry (Quantume Chemistry) in Department of Chemistry, University of Baghdad.

Ahmad Shalaan Alag received B.Sc. degree, is M.Sc. student Physical Chemistry in Department of Chemistry, University of Baghdad